

# Relativistic Astrophysics with Resonant Multiple Inspirals

Naoki Seto<sup>1</sup>, Takayuki Muto<sup>1,2</sup>

<sup>1</sup>*Department of Physics, Kyoto University Kyoto 606-8502, Japan*

<sup>2</sup>*Department of Earth and Planetary Sciences, Tokyo Institute of Technology,  
2-12-1, Oh-okayama, Meguro-ku, Tokyo, 152-8550, Japan*

(Dated: November 5, 2018)

We show that a massive black hole binary might resonantly trap a small third body (*e.g.* a neutron star) down to a stage when the binary becomes relativistic due to its orbital decay by gravitational radiation. The final fate of the third body would be quite interesting for relativistic astrophysics. For example, the parent binary could expel the third body with a velocity more than 10 % of the speed of light. We also discuss the implications of this three-body system for direct gravitational wave observation.

## I. INTRODUCTION

The orbital period of Pluto is 3/2 times that of Neptune, and their mutual stability is maintained by this simple commensurability (termed *the mean motion resonance*). In addition to this well-known fact, the Solar system has various forms of the mean motion resonances [1]. Furthermore, more than 8 exoplanet systems are known to have two planets in mean motion resonances. One of the notable properties here is that once two planets are trapped in a stable resonance relation, they often keep the state for a long time. For example, recent numerical studies showed that some resonant trappings are strong enough to be preserved against planet migration during which orbital radii of two planets decreased by more than 1 order of magnitude [2].

Black hole (BH) binaries are considered as fascinating sources of broad astrophysical phenomena, and, at the same time, their inspirals and mergers are promising targets for gravitational wave (GW) observation that would also provide us with ideal opportunities to test fundamental aspects of gravity. As in the case of planetary systems, a massive BH binary might resonantly trap a small body, *e.g.* through interaction with its surrounding disk, and shrink its orbit by dissipative processes. In this paper we call this kind of three-body system a resonant multiple inspiral (RMI), and study the evolution and the final fate of an RMI, including the post-Newtonian effects. We find that a BH binary has potential to keep a third body down to a stage when the binary becomes relativistic due to its orbital decay by gravitational radiation. We also mention impacts of RMIs on relativistic astrophysics and future GW observation.

## II. STABLE EQUILIBRIUM POINTS

We study the evolution of RMI using a circular restricted three-body problem, namely, analyze the motion of a test particle trapped by a BH binary in a circular orbit with masses  $(1 - \mu)M$  and  $\mu M$  [ $M$ : total mass of the binary,  $\mu (\leq 0.5)$ : the mass ratio]. We use the geometrical unit  $G = c = M = 1$  with which the Schwarzschild radii of the two BHs are  $2(1 - \mu)$  and  $2\mu$  respectively. If

necessary, we intentionally recover the mass parameter  $M$  to show the actual scales of physical quantities. We introduce a parameter  $r_b$  for the binary separation.

In this paper, we concentrate on 1:1 mean motion resonances as tractable but intriguing examples (see *e.g.* [3] for recent related studies). In this case the test particle moves around the equilibrium points  $L_4$  or  $L_5$ . The two points are at almost equilateral positions relative to the parent binary on its orbital plane. After the pioneering work by Lagrange in 1772, various properties have been theoretically investigated for the two points. In the real Universe, the Sun-Jupiter system ( $\mu \sim 10^{-3}$ ) has a large number of asteroids known as Trojans around its  $L_4$  and  $L_5$  (first discovered in 1906) [1, 4], and their origin is still on active debates [4, 5]. Similar objects have been found *e.g.* for the Sun-Mars ( $\mu \sim 2 \times 10^{-7}$ ) or Saturn-Tethys ( $\mu \sim 10^{-6}$ ) systems [1]. Here Tethys is the fifth largest moon of Saturn.

In order to describe the motion of a test particle around  $L_4$  or  $L_5$ , it is convenient to introduce a normalized frame  $(X_N, Y_N, Z_N)$  that is co-rotating with the parent binary around its barycenter. In this frame, the larger BH is at  $(\mu, 0, 0)$ , the smaller one is at  $(-(1 - \mu), 0, 0)$  and their separation is unity. The  $Z_N$  axis is the rotation axis of the parent binary and normal to its orbital plane [24]. Meanwhile, the positions of the two equilibrium points  $L_4$  and  $L_5$  are given by  $(X_L, -Y_L, 0)$  and  $(X_L, Y_L, 0)$  with

$$X_L = -\frac{1}{2} + \mu + \frac{5(-1/2 + \mu)}{4r_b} + o(r_b^{-1}), \quad (1)$$

$$Y_L = \frac{\sqrt{3}}{2} + \frac{6\mu(1 - \mu) - 5}{8\sqrt{3}r_b} + o(r_b^{-1}), \quad (2)$$

where the terms  $\propto r_b^{-1}$  represent the first-order post-Newtonian (1PN) corrections [6, 7].

We briefly summarize the results of the linear stability analysis for a test particle around the equilibrium points  $L_4$  and  $L_5$  [1, 8]. In Newtonian mechanics, small perturbations around these points are given by the superposition of two stable oscillating modes for  $\mu < \mu_1 = 1/2 - \sqrt{69}/18 = 0.038521$  [8]. They are known as the epicyclic motion with the frequency  $\omega_E$  and the libration motion with  $\omega_L (< \omega_E)$  [1]. The two frequencies

are given by

$$\omega_{E,L} = \omega_{BN} \frac{\sqrt{1 \pm \sqrt{1 - 27\mu(1-\mu)}}}{\sqrt{2}} \quad (3)$$

with the orbital frequency of the parent binary  $\omega_{BN} \equiv (M/r_b^3)^{1/2}$  defined at the Newtonian order (correspondence of signs,  $\omega_E : +$  and  $\omega_L : -$ ) [1]. The two frequencies degenerate at  $\mu = \mu_1$ . For a larger mass ratio  $\mu > \mu_1$ , the perturbation becomes unstable.

With 1PN analysis, the two basic frequencies  $\omega_E$  and  $\omega_L$  have the correction terms of  $O(r_b^{-1})$ . It is worth stressing that the ratio  $\omega_E/\omega_L$  now depends not only on the mass ratio  $\mu$  but also on the separation  $r_b$  of the parent binary. The critical mass ratio  $\mu_1$  is given explicitly by  $\mu_1 = 0.03852 - 0.29056M/r_b$  [6].

### III. EVOLUTION OF RMI

An interesting question here is how the resonant trapping changes with the evolution of the parent binary. Below, we numerically study this issue, as a restricted circular three-body problem.

For the evolution of the circular parent BH binary, we can follow its 1PN orbit almost analytically, including the orbital decay by the radiation of GW (see the Appendix for formulations and basic numerical scheme). Gravitational radiation reaction generates a dissipative force starting at 2.5PN order [9]. Below this order, the system is conservative. Since we assume that the mass of the third body (test particle) is negligible, the dissipative evolution is controlled by the motion of the parent binary, through the fifth time derivative of its quadrupole moment. After some algebra, the decrease of the orbital separation of the parent binary is described by the standard expression [9]

$$\frac{dr_b}{dt} = -\frac{64}{5}\mu(1-\mu)\left(\frac{r_b}{M}\right)^{-3}. \quad (4)$$

Accordingly, the rotation cycle  $N$  of the binary before the coalescence is estimated by

$$N = \frac{1}{64\pi\mu(1-\mu)}\left(\frac{r_b}{M}\right)^{5/2}. \quad (5)$$

Given the positions of the parent binary, we can numerically follow the evolution of the test particle. Note that the dissipative acceleration directly works also on the test particle, as easily understood from the fact that the energy loss rate is proportional to the square of the GW amplitude [9]. This effect might induce interesting effects for a 1:1 resonance, due to the apparent phase coherence of the three particles.

Since we cannot properly handle the strong gravity around the two BHs with our 1PN equation of motion, we conservatively terminate our integration when (i) the

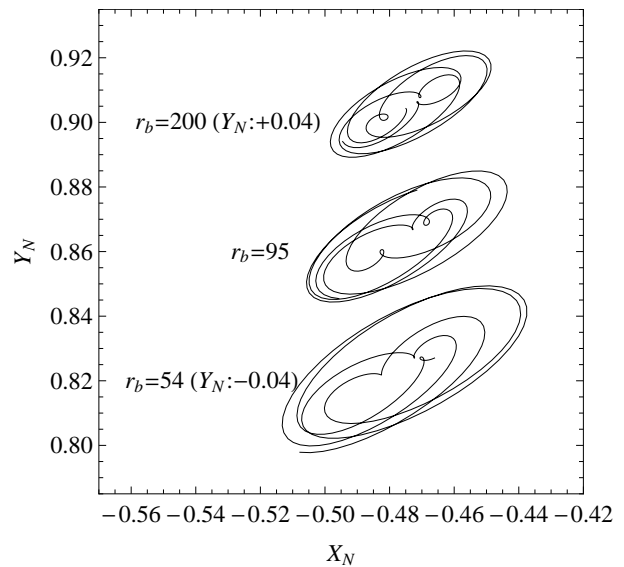


FIG. 1: Evolution of the orbit of a test particle around the  $L_5$  point in the normalized corotating frame  $(X_N, Y_N)$ . The mass ratio of the parent binary is  $\mu = 0.027$ . We show the orbits at three different separations  $r_b = 200, 95$  and  $54$ . Each figure is given for  $\sim 8$  rotation cycles of the parent binary. The initial conditions are  $q_x = 0.002, q_z = 0.001$  at  $r_b = 200$ . The upper and bottom figures are shifted toward the vertical direction by  $\pm 0.004$ .

separation of the parent BH binary reaches the innermost stable circular orbit at  $r_b = 6$  [9] or (ii) similarly, the test particle goes into 3 Schwarzschild radii of each parent BH. As for the initial position and velocity of the test particle, we simply introduce two small parameters  $q_x$  and  $q_z$  related to its position in the corotating frame  $(X_N, Y_N, Z_N)$  as  $(X_L(1+q_x), \pm Y_L, 2X_L q_z)$  with  $X_L$  and  $Y_L$  given in eqs.(1) and (2) at the 1PN order. Here the parameter  $q_x$  sets the perturbation of the third body within the orbital plane of the parent binary, and another one  $q_z$  is related to the inclination with respect to the plane. The particle is released with an initial velocity with which it is at rest in the corotating frame. Note that we made perturbative treatment of the 1PN correction terms. Thus, even with  $q_x = q_z = 0$ , a small initial perturbation of  $O(r_b^{-2})$  is induced around the equilibrium points due to the truncation effect (see *e.g.* [10] for a similar case).

We hereafter discuss the results only from the  $L_5$  region. We have compared the evolution of the test particles starting from both the  $L_4$  and  $L_5$  regions, but have not found notable qualitative differences. In Fig.1 we show the orbits of a test particle at three different epochs. This is a typical example for the evolutionary behavior of the perturbation around the  $L_5$  point. Each figure clearly shows the characteristic profile of a tadpole orbit that is given by the superposition of the two elliptical motions; the short-period epicyclic mode (with the frequency  $\omega_E$ ) and the long-period libration mode (with  $\omega_L$ ) [1].

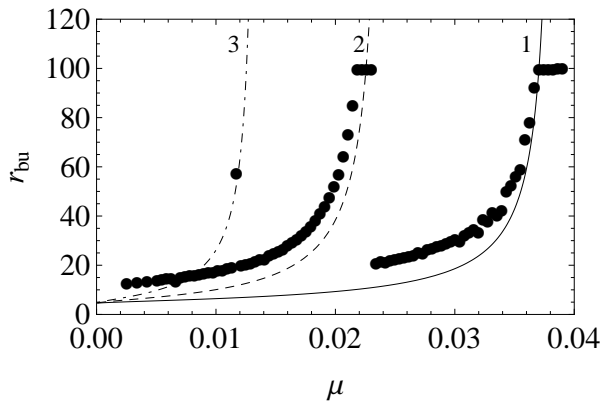


FIG. 2: The unstable separation  $r_{bu}$  of a parent binary as a function of its mass ratio  $\mu$ . The points are given from the evolution of the test particle initially placed around the  $L_5$  point at  $r_b = 100$ . The solid curve is derived from the stability condition  $\omega_L = \omega_E$  at 1PN and has the asymptotic profile  $r_{bu} \rightarrow \infty$  at  $\mu = 0.038521$ . The dashed and dot dashed curves are given for  $\omega_E = 2\omega_L$  and  $\omega_E = 3\omega_L$  with the critical mass ratios  $\mu = 0.024293$  and  $\mu = 0.013516$ , respectively.

With a simplified Hamiltonian and an associated adiabatic invariant [11], Fleming and Hamilton [12] analytically predicted how migration of Jupiter affects the orbital evolution of its Trojan asteroids (with Newtonian mechanics). Since the time scale of gravitational radiation is much larger than the orbital period of the parent BH binary (at least for  $r_b$  given in Fig.1), their analytical prediction might fit with our study. Indeed, the evolution shown in Fig.1 are close to the predicted scaling behavior  $\propto r_b^{-1/4}$  for the trajectories in the normalized corotating frame. Thus we can expect a fairly moderate evolution for the perturbation around the  $L_4$  and  $L_5$  points during the inspiral of the circular parent binary, before its separation becomes small and the unstable modes are generated due to the PN effect as we see next.

For various mass ratio  $\mu$ , we followed a test particle initially with  $q_x = q_z = 0$  at  $r_b = 100$ , and measured the binary separation  $r_{bu}$  where the distance between the test particle and the  $L_5$  point becomes larger than 0.7 (a somewhat arbitrary value) in the normalized corotating frame. In Fig.2, our numerical results are shown by black points. In addition to these results, we examined the unstable separation  $r_{bu}$  starting from finite (but small)  $q_x$  and  $q_z$ , and obtained similar results (see *e.g.* Figs.3 and 4). We also studied the evolution by Newtonian equation of motion, and found that the binary can resonantly hold the test particle typically down to our termination limit at  $r_b = 6$ . In Fig.2, the solid curve represents the 1PN prediction for the binary separation  $r_{bu}$  where the  $L_4$  and  $L_5$  points become unstable (corresponding to the degeneracy condition  $\omega_E = \omega_L$ ). At the regime  $\mu \gtrsim 0.025$ , the unstable radius  $r_{bu}$  shows a reasonable agreement with the analytical result.

Interestingly, our numerical results in Fig.2 show a

strong branch around  $\mu \sim 0.02$ . We found that this is caused by a resonant instability due to the coupling of the epicyclic and libration modes around  $\omega_E = 2\omega_L$ , corresponding to the specific mass ratio  $\mu = 0.024293$  for the Newtonian analysis [13]. With the PN effects, the ratio  $\omega_E/\omega_L$  depends not only on the mass ratio  $\mu$  but also on the binary separation  $r_b$ , as mentioned before. Therefore, even if a parent binary has a mass ratio satisfying  $\omega_E/\omega_L > 2$  at the Newtonian limit  $r_b \rightarrow \infty$ , it could match the unstable condition  $\omega_E/\omega_L = 2$  at a finite  $r_b$  due to the orbital shrink by gravitational radiation. As a result, with the general relativistic effects, the binary is affected by the resonant instability for a broader mass range  $\mu$ , in contrast with a purely Newtonian system.

Figure 2 also shows a branch associated with  $\omega_E = 3\omega_L$  corresponding to the specific mass ratio  $\mu = 0.013516$  for the Newtonian limit [13]. However, this higher-order effect is relatively weak, and many binaries can safely go through the unstable separation, as shown in Fig.2.

#### IV. FINAL FATE OF RMI

As we have studied so far, with RMI, a third body could stay around a parent BH binary deeply into the relativistic regime. Even though careful attention should be paid for interpreting our 1PN results, they would provide us with qualitative insights about the potential final fate of the third body. This issue would be particularly interesting in relation to GW observation with the Laser Interferometer Space Antenna (LISA) [14]. In order to make concrete pictures for LISA, we assume that the total mass of a parent BH binary is  $M \sim 10^6 M_\odot$ , and the mass of the third body is  $\sim 1 - 10 M_\odot$ . Given the stability condition  $\mu < \mu_1 = 0.03852$  for a 1:1 resonance, the parent BH binary might be regarded as an intermediate mass ratio inspiral rather than an inspiral of two comparable BHs. While abundance of BHs around  $\sim 10^4 M_\odot$  is not well known at present, the actual event rate of the former might be higher than that of the latter.

The signal-to-noise ratio of GW associated with the small third body would be much lower than that of the parent BH binary. However, the stronger GW signal from the parent BH binary would enable us to easily estimate the basic parameters of the parent such as the mass ratio  $\mu$  or the total mass  $M$ . Then, for example, from the estimated masses of a potential parent, we can predict the epoch when the  $L_4$  and  $L_5$  points become dynamically unstable (see Fig.2). This kind of prior information would considerably help us to make a careful follow-up data analysis searching for a weaker GW signal by a third body.

Statistical analyses for the final fates of RMIs with realistic initial conditions would be useful for astrophysical arguments, but they are far beyond the scope of this paper. Here, we would rather make qualitative discussions on the expected destinies. Among our numerical samples, ejection of a test particle from the parent binary is a fre-

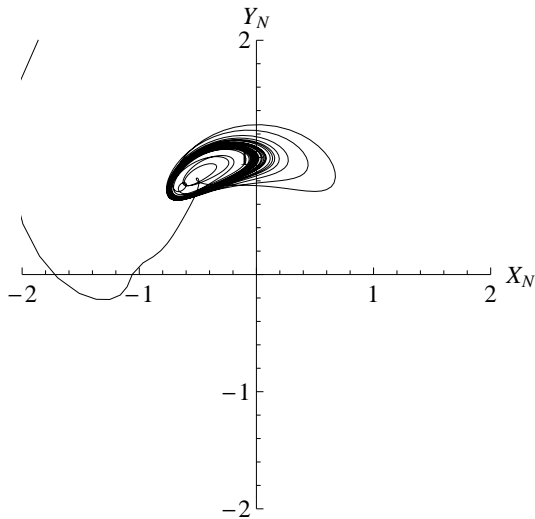


FIG. 3: Ejection of a test particle around the binary separation  $r_b = 24.6$  after  $N \sim 1.1 \times 10^5$  cycles from  $r_b = 200$ . The ejection velocity is  $\sim 0.14c$ . The initial conditions are the same as Fig.1. The larger BH is at  $(0.027, 0, 0)$  and the smaller one is at  $(-0.973, 0, 0)$ . They rotate counterclockwise.

quent final state. In Fig.3, we show the trajectory of the test particle evolved from Fig.1. The  $L_5$  point becomes dynamically unstable around  $r_b \sim 24.6$  and the particle was soon scattered by the smaller BH at  $(-0.973, 0, 0)$ . It escaped from the binary with a terminal velocity of  $\sim 0.14c$ , which is much larger than the typical kick velocity by the anisotropic GW emission [15]. For an RMI event, the third body can be scattered by a relativistic binary, and this magnitude is not surprising. The third body should be a neutron star or a black hole for surviving tidal disruption during the large angle scattering by the smaller BH of the parent binary.

Though an electromagnetic wave search for such a high velocity object would be challenging, we might get a signature of its ejection by careful analysis of GWs. If the third body is a white dwarf and tidal disruption occurs, we might observe a short-period electromagnetic wave signal before the merger of the parent BH binary. This might help us to identify its host galaxy and perform cosmological studies, *e.g.* constraining dark energy parameters through the relation between the redshift and the luminosity distance of the binary [16].

From our numerical samples, we expect that a plunge into the larger BH would be another likely scenario. Note that, from a distance of  $O(r_{bu})$ , its angular size is much larger than a degree scale. For a plunge into the smaller one, we might detect its GW signal by ground-based detectors, depending on the mass of the BH.

Some of our numerical samples resulted in the dynamical formation of extreme-mass-ratio-inspiral (EMRI) systems. In Fig.4, we present the trajectory of a test particle around the unstable separation  $r_b \sim 13$ . After the transitional stage shown in Fig.4, the test particle almost

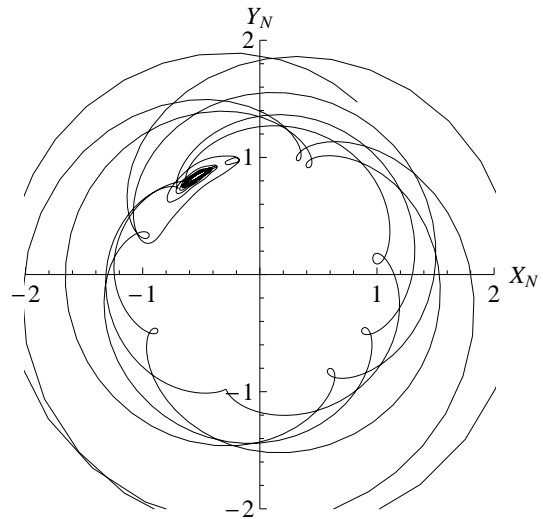


FIG. 4: Dynamical formation of an EMRI system around  $r_b = 13.0$  with  $\mu = 0.0025$ . The initial positions are  $q_x = 0.004$  and  $q_z = 0.08$  at  $r_b = 77$  ( $9.9 \times 10^4$  cycles to  $r_b = 13.0$ ).

decouples from the evolution of the parent BH binary. When the binary reach the innermost stable circular orbit  $r_b = 6$ , we have an eccentric EMRI system with pericenter distance  $\sim 13$  and the apocenter distance  $\sim 50$ . GW from an EMRI is a very important target of LISA for directly probing highly distorted geometry around BHs, although we need significant effort to detect it due to its complicated waveform and the limitation of available computational power [17]. As we commented earlier, the basic parameters of the parent BH would be estimated by its stronger but simpler GW signal. Thus the subsequent EMRI signal would be detected more easily than a blind EMRI search as usually assumed. Furthermore, we might, in principle, use the third body to probe the dynamical gravitational field caused by the merger of the parent BH binary to precisely measure the basic parameters (*e.g.* mass and spin) of the merged BH.

## V. DISCUSSIONS

Our study for RMIs is based on the 1PN restricted three-body analysis for a circular parent binary. This simple treatment can be extended in diverse ways. One of the principle directions is to include higher-order PN effects and spins of BHs. A complementary approach would be to inject a test particle into a numerically evolved BH binary (for recent breakthrough see [18]). From Newtonian analyses we expect that modest eccentricity ( $e \lesssim 0.1$ ) of the parent binary would not largely change our basic results [19], but this should be checked specifically. Meanwhile, we have regarded the third body as a massless pointlike particle. Actually, the assumption for the mass would be largely relaxed for RMIs [8]. For example, Saturn has stable co-orbital satellites (in

a 1:1 resonance); Janus and Epimetheus whose masses are comparable (1:0.25) [1]. Furthermore, the internal structure of the third body might cause interesting astrophysical effects (*e.g.* for a main-sequence star or even a gas cloud). Beyond a three-body problem, a parent BH binary might keep many small objects around its  $L_4$  and  $L_5$  points, similar to the Trojan asteroids of the Sun-Jupiter system. In the case of a 1:1 resonance, we have a severe upper limit  $\mu < \mu_1$  for the restricted three-body problem, but a larger mass ratio might be allowed for resonances other than 1:1.

In addition to these refinements for the evolution of RMIs, follow-up studies in related fields are worth ex-

ploring. More detailed analyses for detectability of GW signatures at various stages of RMIs would be fruitful, especially for space interferometers such as LISA. Finally, discussions on the formation mechanism of RMIs would be an attractive topic on astrophysics (see *e.g.* [20] and references there in for related studies).

The authors would like to thank H. Arakida and K. Tomida for their kind support. This work was supported by the Grant-in-Aid for the Global COE Program "The Next Generation of Physics, Spun from Universality and Emergence" from the Ministry of Education, Culture, Sports, Science and Technology (MEXT) of Japan.

- 
- [1] C. D. Murray and S. F. Dermott, *Solar System Dynamics* (Cambridge University Press, UK, 1999).
  - [2] A. T. Lee, E. W. Thommes and F. A. Rasio, *Astrophys. J.* **691**, 1684 (2009).
  - [3] Z. E. Wardell, arXiv:gr-qc/0206059; H. Asada, *Phys. Rev. D* **80**, 064021 (2009).
  - [4] F. Marzari et al. in *Asteroids III*, edited by W. F. Bottke et al. (University of Arizona Press, Tucson, 2002) p.725.
  - [5] A. Morbidelli et al. *Nature*, **435**, 462 (2005).
  - [6] T. I. Maindl and H. Hagel, in *Proceedings of the 3rd International Workshop on Positional Astronomy and Celestial Mechanics*, edited by A. Lopez Garcia et al. (1996), p.183.
  - [7] E. Krefetz, *Astron. J.*, **72**, 471 (1967).
  - [8] M. Gascheau, *Comptes Rendus*, **16**, 393 (1843).
  - [9] L. D. Landau and E. M. Lifshitz, *The Classical Theory of Fields* (Pergamon Press, Oxford, 1971).
  - [10] C. O. Lousto and H. Nakano, *Class. Quant. Grav.* **25**, 195019 (2008).
  - [11] L. D. Landau and E. M. Lifshitz, *Mechanics* (Pergamon Press, Oxford, 1969).
  - [12] H. J. Fleming and D. P. Hamilton, *Icarus*, **148**, 479 (2000).
  - [13] A. Deprit, and A. Deprit-Bartholome, *Astron. J.*, **72**, 173 (1967).
  - [14] P. L. Bender et al. LISA Pre-Phase A Report, Second edition (1998).
  - [15] J. G. Baker, et al. *Astrophys. J.* **653**, L93 (2006); M. Campanelli, et al. *Phys. Rev. Lett.* **98**, 231102 (2007).
  - [16] B. F. Schutz, *Nature* **323**, 310 (1986).
  - [17] J. R. Gair, et al. *Class. Quant. Grav.* **21**, S1595 (2004).
  - [18] F. Pretorius, *Phys. Rev. Lett.* **95**, 121101 (2005); M. Campanelli et al. *Phys. Rev. Lett.* **96**, 111101 (2006); J. G. Baker et al. *Phys. Rev. Lett.* **96**, 111102 (2006).
  - [19] A. Bennett, *Icarus*, **4**, 177 (1965).
  - [20] M. Fujii, M. Iwasawa, Y. Funato and J. Makino, arXiv:1003.4125 [astro-ph.GA].
  - [21] S. Chandrasekhar and G. Contopoulos, *Proc. Roy. Soc. of London. A*, **298** Issue 1453, 123 (1967).
  - [22] W. H. Press et al. *Numerical Recipes in Fortran 90* (Cambridge University Press, Cambridge, 1996).
  - [23] T. I. Maindl and R. Dvorak, *Astron. Astrophys.*, **290**, 335, (1994).
  - [24] With respect to the coordinate system defined in Fig.3.1 of [1], we have the correspondences  $X_n:-x$ ,  $Y_N:y$  and

$Z_N:z$ .

## Appendix A: equations of motion for particle systems

In this Appendix, we briefly explain the basic equations applied in our numerical calculations for dynamical evolution of RMI. For the conservative 1PN equations of motion, we use the Hamiltonian form of the Einstein-Infeld-Hoffman Lagrangian given for a point-particle system with masses  $m_a$  ( $a$ : the label for particles) [9, 21]. We follow the positions  $x_{ai}$  ( $i = 1, 2, 3$ : the label for spatial directions) in the barycentric non-rotating frame ( $x_1, x_2, x_3$ ). Rather than adopting the standard conjugate momenta  $p_{ai}$ , we introduce the new variables

$$s_{ai} \equiv \frac{p_{ai}}{m_a} \quad (\text{A1})$$

that are convenient for dealing with restricted three-body problems. Our 1PN Hamiltonian is expanded as

$$H = H_N + H_{1PN} \quad (\text{A2})$$

with the explicit forms of the Newtonian and 1PN terms

$$H_N = \frac{1}{2} \sum_a m_a s_a^2 - \frac{1}{2} \sum_{a,b \neq a} \frac{m_a m_b}{r_{ab}} \quad (\text{A3})$$

$$\begin{aligned} H_{1PN} = & -\frac{1}{8} \sum_a m_a (s_a^2)^2 + \frac{1}{2} \sum_{a,b \neq a, c \neq a} \frac{m_a m_b m_c}{r_{ab} r_{ac}}, \\ & + \frac{1}{4} \sum_{a,b \neq a} \frac{m_a m_b}{r_{ab}} \{-6s_a^2 + 7\mathbf{s}_a \cdot \mathbf{s}_b \\ & + (\mathbf{n}_{ab} \cdot \mathbf{s}_a)(\mathbf{n}_{ab} \cdot \mathbf{s}_b)\}, \end{aligned} \quad (\text{A4})$$

where  $r_{ab} = |\mathbf{x}_a - \mathbf{x}_b|$  and  $\mathbf{n}_{ab} = (\mathbf{x}_a - \mathbf{x}_b)/r_{ab}$ .

For our new set of variables ( $x_{ai}, s_{ai}$ ), the canonical equations are modified as follows;

$$\frac{ds_{ai}}{dt} = -\frac{1}{m_a} \frac{\partial H}{\partial x_{ai}}, \quad \frac{dx_{ai}}{dt} = \frac{1}{m_a} \frac{\partial H}{\partial s_{ai}}. \quad (\text{A5})$$

These are well behaved in the limit  $m_a \rightarrow 0$  for a restricted problem. Note that with the 1PN terms the simple identity  $s_{ai} = \frac{dx_{ai}}{dt} (\equiv v_{ai})$  does not hold, and we have the following correspondence at the 1PN order [21];

$$s_{ai} = v_{ai} + v_{ai} \left( \frac{v_a^2}{2} + 3 \sum_{b \neq a} \frac{m_b}{r_{ab}} \right) - \frac{1}{2} \sum_{b \neq a} \frac{m_b}{r_{ab}} \{ 7v_{bi} + (\mathbf{n}_{ab} \cdot \mathbf{v}_b) n_{abi} \}. \quad (\text{A6})$$

In this paper, we study circular restricted three-body problems in which the massless third body is irrelevant for the evolution of the parent binary (with masses  $m_1$  and  $m_2$ ). The dynamics of the circular parent binary is characterized by the orbital frequency  $\omega_b$  as a function of the binary separation  $r_b \equiv |\mathbf{x}_1 - \mathbf{x}_2|$ , and it is perturbatively expressed as

$$\omega_B = \omega_{BN} + \omega_{B1PN} \quad (\text{A7})$$

with the Newtonian result

$$\omega_{BN} = \left\{ \frac{m_1 + m_2}{r_b^3} \right\}^{1/2}. \quad (\text{A8})$$

Applying the above Hamiltonian for two particles, we obtain the 1PN correction term as (see *e.g.* [7])

$$\omega_{B1PN} = \omega_{BN} \frac{m_1 + m_2}{2r_b} \left\{ \frac{m_1 m_2}{(m_1 + m_2)^2} - 3 \right\}. \quad (\text{A9})$$

Thus the motion of the parent binary can be handled analytically, and we can numerically follow the position of the third body with the modified canonical equations, plugging in the analytical information of the parent binary.

Up to now, our 1PN system is conservative and this will provide us with a good opportunity to check the

accuracy of our numerical code (based on a fifth order Runge-Kutta integration scheme [22]) for the motions of third bodies around the Lagrange points. For relevant sets of parameters ( $r_b, \mu, q_x$ ), we examined the 1PN version of Jacobi energy derived for motions of the third body within the orbital plane of the parent binary [23]. We found that it is typically conserved by  $\sim 10^{-5}$  level for  $\sim 10^5$  orbital rotation cycles.

Finally we summarize the dissipative effects caused by gravitational radiation. The first equation of (A5) is now modified as follows

$$\frac{ds_{ai}}{dt} = -\frac{1}{m_a} \frac{\partial H}{\partial x_{ai}} + \left( \frac{ds_{ai}}{dt} \right)_{rad}, \quad (\text{A10})$$

where the second term is due to the radiation, and at the lowest order, it is given by

$$\left( \frac{ds_{ai}}{dt} \right)_{rad} = -\frac{2}{15} D_{ij}^{(V)} x_{aj}. \quad (\text{A11})$$

Here  $D_{ij}^{(V)}$  is the fifth time derivative of the quadrupole moment  $D_{ij}$  defined by [9]

$$D_{ij} \equiv \sum_a m_a (3x_{ai} x_{aj} - x_a^2 \delta_{ij}). \quad (\text{A12})$$

For the restricted three body-problem, the moment  $D_{ij}$  is determined only by the parent circular binary ( $a = 1, 2$ ), and its fifth time derivative is evaluated analytically with a standard adiabatic treatment. After some algebra, we obtain the time derivative of the separation  $r_b$  of the parent binary as in Eq.(4), and its orbital position is determined straightforwardly. Then, with a method similar to the previous conservative case, we can numerically follow the massless third body. Our numerical results in Sec.III-IV are obtained in this manner.